

The semiclassical and quantum regimes of super-radiant light scattering from a Bose–Einstein condensate

G R M Robb¹, N Piovella² and R Bonifacio²

¹ Department of Physics, University of Strathclyde, 107 Rottenrow, Glasgow G4 0NG, UK

² Dipartimento di Fisica, Università degli Studi di Milano, INFN and INFN, Via Celoria 16, Milano I-20133, Italy

E-mail: g.r.m.robb@strath.ac.uk and nicola.piovella@mi.infn.it

Received 4 October 2004, accepted for publication 10 February 2005

Published 9 March 2005

Online at stacks.iop.org/JOptB/7/93

Abstract

We show that many features of the recent experiments of Schneble *et al* (2003 *Science* **300** 475), which demonstrate two different regimes of light scattering by a Bose–Einstein condensate, can be described using a one-dimensional mean-field quantum CARL model, where optical amplification occurs simultaneously with the production of a periodic density modulation in the atomic medium. The two regimes of light scattering observed in these experiments, originally described as ‘Kapiza–Dirac scattering’ and ‘super-radiant Rayleigh scattering’, can be interpreted as the semiclassical and quantum limits respectively of CARL lasing.

Keywords: BEC, super-radiance, CARL, recoil, collective, Kapiza–Dirac

(Some figures in this article are in colour only in the electronic version)

1. Introduction

The study of nonlinear optical phenomena arising from the collective motion of atoms in dynamic optical fields has been an active field of predominantly theoretical research over the last decade. A large fraction of this work has been concerned with the collective atomic recoil laser (CARL) [1–6]. As part of the continuing progress in the production and investigation of ultracold atomic gases and Bose–Einstein condensates (BECs), there have been several experiments which have demonstrated the validity of these models and realized some of their predictions. Examples include the observation of collective atomic recoil lasing by a cold thermal gas in a high-finesse cavity [7, 8] and the observation of super-radiant Rayleigh scattering by a BEC [9–11]. Super-radiant Rayleigh scattering involves the production of pulses of coherently scattered radiation simultaneous with the splitting of the condensate into discrete momentum groups due to atomic recoil. Several theoretical models have been used to describe the evolution of the super-radiant scattering process [4–6, 12–15], including an extension of the original classical

CARL model [1–3] to include a quantum treatment of the atomic dynamics [5, 6, 13]. Recent experimental work by Schneble *et al* [16] has shown that in addition to the super-radiant Rayleigh scattering process originally observed in [9], there is a second scattering regime termed ‘Kapiza–Dirac scattering’. During super-radiant Rayleigh scattering, the scattering process involves only emission of scattered photons i.e. absorption of pump photons and emission of scattered (probe) photons. In contrast, during Kapiza–Dirac scattering the scattering process involves both emission *and absorption* of scattered (probe) photons i.e. absorption of probe photons and emission of pump photons.

In this paper it is shown that many features of the recent experiments of Schneble *et al* [16] can be described using a one-dimensional mean-field quantum CARL model, where optical amplification occurs simultaneously with the production of a periodic density modulation in the atomic medium. Using this model, we demonstrate that the two regimes of ‘Kapiza–Dirac scattering’ and ‘super-radiant Rayleigh scattering’ observed in [16] can be interpreted as the semiclassical and quantum limits respectively of CARL lasing.

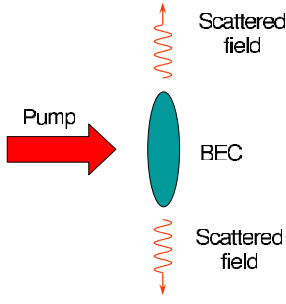


Figure 1. Schematic diagram illustrating the geometry of the super-radiant scattering experiments of [16, 9].

It will be shown that the two regimes are distinguished by the relative size of the gain of the super-radiant scattering process and the frequency separation of the absorption and emission peaks. A significant difference between the results presented here and those of other theoretical models of the experiments of Schneble *et al* [16, 17] is that in this model the regime of scattering is not determined by the pump pulse duration, so the scattering process does not evolve in time from one to the other.

2. Model

The model used to describe the BEC–light interaction is the mean-field quantum CARL model originally derived in [5, 6]. The model is one dimensional and describes the evolution of a backscattered (probe) field arising from scattering of a pump laser field (assumed to be of constant amplitude) by an elongated BEC. In the experiments of Schneble *et al* [16], the geometry of the experiment is essentially two dimensional, as illustrated schematically in figure 1 with emission of two endfire modes from each end of the long axis of the condensate, propagating transversely to the pump laser. If we assume that coupling between the endfire modes (which are much weaker than the pump) is negligible, each endfire mode can be assumed to evolve independently and the atomic motion is one dimensional.

When the pump laser is sufficiently detuned from the atomic resonance, it leaves the atoms in the internal ground state. Consequently, radiation pressure due to absorption and subsequent random incoherent, isotropic emission of a photon can be neglected. In this detuned regime, coherent scattering of the pump laser is the dominant process. The atoms interact with a laser beam of wavevector \vec{k} and scatter photons of wavevector \vec{k}_s , recoiling with a momentum $\hbar\vec{q} = \hbar(\vec{k} - \vec{k}_s)$. The atoms, initially scattered randomly into various momentum states, interfere with the atoms in the original momentum state. This creates a matter wave grating having the correct periodicity to further scatter the laser beam in the direction \vec{k}_s . In an elongated condensate a preferential direction for the scattered photons emerges, causing super-radiant Rayleigh scattering. Both the matter wave grating and the scattered light are coherently amplified [9, 16].

In a simplified 1D description of the process along the direction of the atomic recoil momentum $\hbar\vec{q}$, the evolution of the matter wave field $\Psi(\theta, t)$ and of the dimensionless amplitude $a(t)$ of the scattered radiation is determined by the

following quantum mean-field CARL model [5, 6]:

$$i\frac{\partial\Psi}{\partial t} = -\omega_r\frac{\partial^2\Psi}{\partial\theta^2} - ig[ae^{i(\theta+\delta t)} - \text{c.c.}]\Psi + \beta|\Psi|^2\Psi \quad (1)$$

$$\frac{da}{dt} = gN \int d\theta |\Psi|^2 e^{-i(\theta+\delta t)} - \kappa a \quad (2)$$

where $\theta = qz$ (with $q = |\vec{q}| \approx \sqrt{2}k$), $a = (\epsilon_0 V/2\hbar\omega_s)^{1/2}E$ is the dimensionless electric field amplitude of the scattered beam with frequency ω_s , $\omega_r = \hbar q^2/2m$ is the two-photon recoil frequency, $g = (\Omega/2\Delta)(\omega d^2/2\hbar\epsilon_0 V)^{1/2}$ is the coupling constant, $\Omega = dE_p/\hbar$ is the Rabi frequency of the laser field with constant amplitude E_p and frequency $\omega = ck$, $\Delta = \omega - \omega_0$ is the detuning from atomic resonance ω_0 , $d = \hat{\epsilon} \cdot \vec{d}$ is the electric dipole moment of the atom along the polarization direction $\hat{\epsilon}$ of the laser, $V = AL$ is the volume of the condensate, A is its cross-sectional area, L is its length, N is the total number of atoms, and $\delta = \omega - \omega_s$. The matter wave field is normalized such that $\int_{-\infty}^{+\infty} d\theta |\Psi|^2 = 1$. The second term on the right-hand side of equation (1) is the self-consistent optical lattice, resulting from the interference between the laser and the scattered radiation, whose amplitude is amplified by the matter wave grating described by the first term on the right-hand side of equation (1) describes the mean-field effect of the atom–atom interaction due to binary collisions, where $\beta = 8\pi\hbar qa_s N/mA$ and a_s is the scattering length. Equation (2) has been written in the ‘mean-field’ limit, which models propagation of light with respect to the atoms by replacing the non-uniform amplitude by its average value and by adding to the equation a damping term with a decay rate $\kappa \approx c/2L$ of the order of the inverse of the photon flight time through the condensate.

Notice that the interaction time t appearing in equations (1) and (2) is the pump field duration, so that our model is suitable to explore both super-radiant Rayleigh scattering (‘long pump pulse duration’) and the self-stimulated Kapitza–Dirac diffraction regime (‘short pump pulse duration’) investigated in [16]. It will be shown here that the relevant parameter in these experiments is not the pump pulse duration but the characteristic time of the optical/matter–wave amplification process, given by the inverse of the gain rate.

If we assume that the atomic wavefunction is periodic on the scale of the optical potential, with spatial period $2\pi/q = \lambda/\sqrt{2}$ which corresponds to a period in θ of 2π , then we can expand the atomic wavefunction in a Fourier series

$$\Psi(\theta, t) = \sum_{n=-\infty}^{\infty} c_n(t) e^{in(\theta+\delta t)}. \quad (3)$$

Furthermore, we assume that the condensate is sufficiently dilute such that $4\pi\hbar a_s n_s/m \ll \omega_r$, where n_s is the average atomic density, so that the atom–atom interaction term in equation (1) may be neglected. The effect of the atom–atom term on the collective recoil lasing has been investigated in [18].

Substituting for $\Psi(\theta, t)$ using equation (3), it can be shown [5, 6, 12] that equations (1) and (2) can be rewritten as

$$\frac{dc_n}{dt} = -in(\omega_r n + \delta)c_n - g(ac_{n-1} - a^*c_{n+1}) \quad (4)$$

$$\frac{da}{dt} = gN \sum_{n=-\infty}^{\infty} c_n c_{n-1}^* - \kappa a. \quad (5)$$

In this quantum description, the Fourier expansion (3) is equivalent to expanding the wavefunction $\Psi(\theta, t)$ in the set of momentum eigenstates with eigenvalues $\vec{p} = (\hbar\vec{q})n$ and $p_n = |c_n|^2$ is the probability for an atom to have a momentum $\vec{p} = (\hbar\vec{q})n$.

In the super-radiant regime explored in the experiments of [9–11, 16], the radiation damping rate κ is always much larger than the gain rate and/or the recoil frequency ω_r , so that the field amplitude follows the atomic motion adiabatically. Hence, neglecting the time derivative, equation (5) yields

$$a \approx \frac{gN}{\kappa} \sum_{n=-\infty}^{\infty} c_n c_{n-1}^*. \quad (6)$$

3. The semiclassical and quantum limits of the super-radiant regime

In order to obtain the gain coefficient of the super-radiant process in the semiclassical and quantum limits from the dynamical equations, let us consider the initial equilibrium state with no field, $a = 0$, and all the atoms at rest, i.e. in the momentum state $n = 0$, with $c_0 = 1$ and $c_m = 0$ for all $m \neq 0$. Linearizing around this equilibrium solution and neglecting the small detuning δ between the laser and scattered frequencies, equations (4) and (6) reduce to the single linear equation for $B = c_1 + c_{-1}^*$:

$$\frac{d^2 B}{dt^2} + \omega_r(\omega_r - iG)B = 0, \quad (7)$$

where G is the super-radiant gain

$$G = \frac{2g^2 N}{\kappa} = \frac{\hbar\omega\Gamma\Gamma_{sc}N}{2AI_{sat}}, \quad (8)$$

Γ is the natural linewidth, $\Gamma_{sc} = \Gamma(\Omega/2\Delta)^2$ is the Rayleigh scattering rate and $I_{sat} = c\hbar^2\Gamma^2/4d^2$ is the saturation intensity. Equation (8) coincides with the super-radiant gain coefficient reported in equation (4) of [16].

It is easy to show that equation (7) has an unstable solution $B(t) \propto \exp[(\lambda_1 + i\lambda_2)t]$, with

$$\lambda_1 = \left(\frac{\omega_r \sqrt{\omega_r^2 + G^2} - \omega_r^2}{2} \right)^{1/2} \quad (9)$$

and $\lambda_2 = \omega_r G/2\lambda_1$. Furthermore, it is easy to show, from equation (7), that

$$\frac{|c_1|}{|c_{-1}|} \approx \frac{G/2}{\sqrt{(\lambda_1 + G/2)^2 + (\lambda_2 + \omega_r)^2}}. \quad (10)$$

These expressions show that the instability may have a semiclassical or quantum character, depending on the ratio between the super-radiant gain G and the recoil frequency ω_r . In fact, in the limit where $G \ll \omega_r$, equations (9) and (10) give $\lambda_1 \approx G/2$, $\lambda_2 \approx \omega_r$ and $|c_1|/|c_{-1}| \approx G/(4\omega_r) \ll 1$. In this limit, the SR process is quantum in nature, with only the lower state $n = -1$ being populated, and the SR gain is G [5, 12].

In the opposite limit in which $G \gg \omega_r$, equations (9) and (10) give $\lambda_1 \approx \lambda_2 \approx \sqrt{\omega_r G/2}$ and $|c_1|/|c_{-1}| \approx 1 - \sqrt{2\omega_r/G}$. In this limit, the SR process is semiclassical in nature, with the states $n = 1$ and -1 almost equally populated. In this case, the super-radiant gain is given by [4]

$$G' = \sqrt{2\omega_r G} = 2g\sqrt{\frac{\omega_r N}{\kappa}}. \quad (11)$$

The SR gain in the semiclassical limit is always lower than the SR gain in the quantum limit, since $G'/G = \sqrt{2\omega_r/G} \ll 1$. Notice also the different dependence of the SR gain on N in the quantum and the classical limits.

4. Numerical results

In order to observe the behaviour of the collective scattering process in the nonlinear regime, equations (4) and (5) were integrated numerically with initial conditions $a = 0$, $c_{-1} = 1/\sqrt{N}$, $c_0 = \sqrt{1-1/N}$, and $c_m = 0$ when $m \neq -1, 0$ and with parameters corresponding to the semiclassical and quantum regimes of evolution. These parameters correspond to the experiments of [16], i.e. a ^{87}Rb condensate illuminated by a pump beam of wavelength $\lambda = 780$ nm and an intensity of 63 mW cm $^{-2}$. The pump couples to the $5S_{1/2} \rightarrow 5P_{3/2}$ transition which has a natural width $\Gamma = 0.37 \times 10^8$ s $^{-1}$, dipole moment $d = 2.07 \times 10^{-29}$ C m, saturation intensity $I_{sat} = 2.5$ mW cm $^{-2}$ and recoil frequency $\omega_r = 4.7 \times 10^4$ s $^{-1}$. The condensate had a cigar-shaped form, 15 μm in diameter and 200 μm in length, so that $\kappa = 7.5 \times 10^{11}$ s $^{-1}$. Using these parameters, the quantum and classical super-radiant gain coefficients of equations (8) and (11) are $G \approx 4.9 \times 10^6 \times N/|\Delta|^2$ and $G' \approx 6.8 \times 10^5 \times \sqrt{N}/|\Delta|$, respectively, where Δ is the pump–atom detuning in megahertz. We assume that $\delta = 0$ and that half of the atoms in the condensate participate in each of two super-radiant emissions along the main axis of the condensate and that the number of atoms participating in the collective scattering process is $N = 10^5$ rather than $N = 10^6$ as quoted for the number of atoms in the condensate in [16]. Qualitative support for this assumption is provided by figure 3(A) of [16], which shows that a large fraction of the condensate atoms do not participate in the coherent super-radiant scattering process. From [16], the ‘Kapiza–Dirac’ experiment was carried out using $\Delta = -420$ MHz, so that $g = 3.2 \times 10^6$ s $^{-1}$ and the quantum super-radiant gain is $G = 3 \times 10^6$ s $^{-1}$. Consequently, the collective scattering process is semiclassical in nature, since $G/\omega_r \sim 58$. For the experiments in the ‘super-radiant Rayleigh scattering’ regime, $\Delta = -4400$ MHz, $g = 3.07 \times 10^5$ s $^{-1}$ and the quantum super-radiant gain coefficient is $G = 2.5 \times 10^4$ s $^{-1}$, so that the collective scattering process is quantum mechanical in nature, since $G/\omega_r \sim 0.53$.

Figure 2 shows snapshots of the atomic momentum distribution at different times for the semiclassical case with $\Delta = -420$ MHz. It can be seen from figure 2(a) that, in agreement with our theory, at the beginning of the interaction momentum states $n = 1$ and -1 are the only non-zero momentum states to have significant population, with $p_1 \sim p_{-1}$, where $p_n = |c_n|^2$. Equation (10) predicts a ratio $|p_1|/|p_{-1}| \approx 0.7$. As time progresses, many momentum states

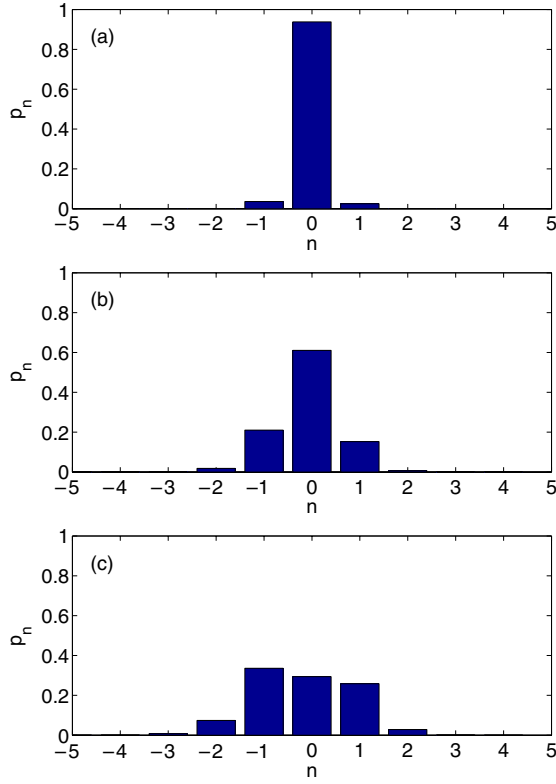


Figure 2. Atomic momentum distribution in the semiclassical regime with $G = 58\omega_r$, when (a) $t = 11 \mu\text{s}$, (b) $t = 15 \mu\text{s}$ and (c) $t = 17 \mu\text{s}$.

with both positive *and* negative n are populated. However, the momentum distribution is not symmetric about $n = 0$. The average momentum is less than zero, so from momentum conservation there is a net gain of the scattered radiation field, shown in figure 3, due to the difference in photon absorption and emission rates. Figure 3 shows that amplification of the scattered field in the semiclassical case is simultaneous with the growth of a strong density modulation in the condensate, as represented by the bunching parameter, $b \equiv \langle e^{-i\theta} \rangle = \sum_n c_n c_{n-1}^*$. The atomic momentum distributions shown in figure 2 are similar to the time-of-flight images observed for the so-called ‘Kapiza–Dirac scattering’ observed in [16], where population of momentum states due to absorption *and* emission of radiation was observed.

Figure 4 shows snapshots of the atomic momentum distribution at different times for the quantum case with $\Delta = -4400$ MHz. It can be seen from figure 4(a) that, in agreement with our model, at the beginning of the interaction momentum state $n = -1$ is the only non-zero momentum state to have significant population, and that the population $p_1 \approx 0$. Equation (10) predicts a ratio $|p_1|/|p_{-1}| \approx 0.01$. As time progresses, the atomic population moves sequentially, $n = -1 \rightarrow n = -2 \rightarrow \dots$, and states with $n > 0$ are never populated. This sequential decrease in atomic momentum gives rise to amplification of the scattered radiation field and again occurs simultaneously with the development of a strong density modulation in the condensate, as shown in figure 5. In contrast to the semiclassical case, however, this amplification of the scattered field occurs due to emission of scattered (probe) photons *only*, and the spread in atomic momenta is much

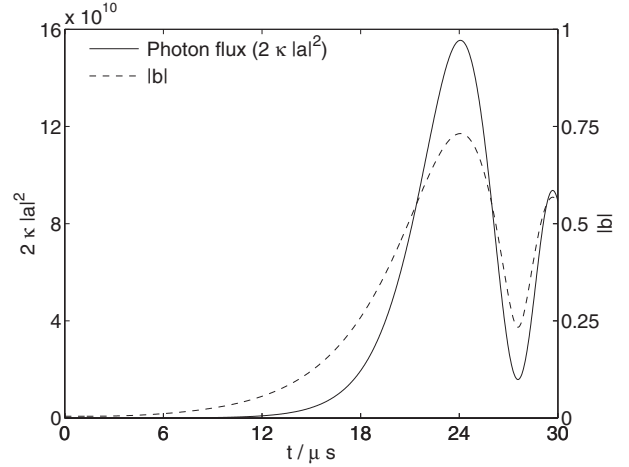


Figure 3. Flux of scattered photons, $2\kappa|a|^2$, and bunching factor, $|b|$, as a function of time in the semiclassical regime with $G = 58\omega_r$.

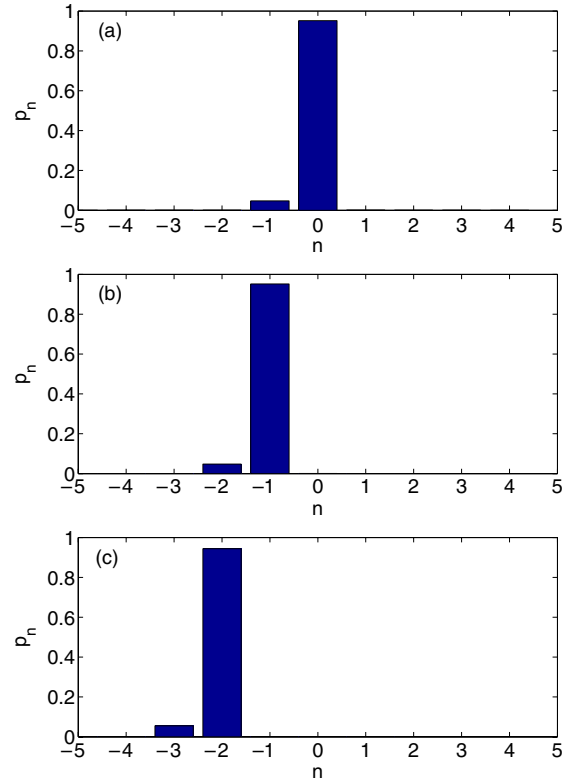


Figure 4. Atomic momentum distribution in the quantum regime with $G = 0.53\omega_r$ when (a) $t = 0.3$ ms, (b) $t = 1.0$ ms and (c) $t = 1.7$ ms.

smaller than in the semiclassical case. The atomic momentum distributions shown in figure 4 are similar to the time-of-flight images observed for ‘super-radiant Rayleigh scattering’ in [16, 9], where the atoms attain momentum *only* in the direction of the pump beam in discrete units of $\hbar\vec{q}$.

5. Interpretation

In [16], the Kapiza–Dirac scattering regime and the super-radiant Rayleigh scattering regime are described as the ‘short-pump-pulse’ and ‘long-pump-pulse’ limits respectively.

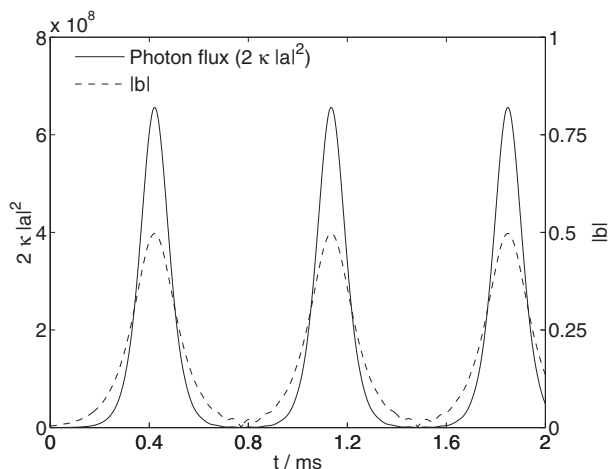


Figure 5. Flux of scattered photons, $2\kappa|a|^2$, and bunching factor, $|b|$, as a function of scaled time in the quantum regime with $G = 0.53\omega_r$.

A problem with this classification is that it implies that for sufficiently long pump pulses the collective scattering makes a transition from Kapitza–Dirac scattering to super-radiant Rayleigh scattering, or in the terminology of this paper a transition from the semiclassical to the quantum regime of CARL lasing. The results presented here however do not support this interpretation. They suggest that the distinguishing feature between the two experiments in [16] is not the pump pulse duration, but the atom–field detuning (which differs by an order of magnitude in the experiments of [16]), which determines the atom–field coupling and consequently the timescale of the super-radiant scattering process. Rather than the ratio of the pump pulse duration relative to the two-photon recoil time (the inverse of the two-photon recoil frequency), it is the size of the super-radiant decay time relative to the two-photon recoil time which determines whether or not the scattering consists of a sequence of emission processes, as observed in the ‘super-radiant Rayleigh scattering’ regime [16, 9], or simultaneous emission and absorption processes, as observed in the ‘Kapitza–Dirac regime’.

A simple justification for this argument is as follows. The atoms are assumed to all be in the condensate initially, so that $p_0 = 1$. The frequencies at which the probabilities of absorption ($n = 0 \rightarrow n = 1$) and emission ($n = 0 \rightarrow n = -1$) are maximum are non-degenerate and differ by a frequency of $2\omega_r$. A transition from ($n = 0 \rightarrow n = -1$) will initiate super-radiant or superfluorescent decay. The characteristic time of the super-radiant decay is $\tau_{sr} \sim G^{-1}$ for $\kappa \gg g\sqrt{N}$ [6], so the spectral width of the super-radiant pulse is $\sim G = 2g^2N/\kappa$. If the spectral width of the SR pulse is much less than the absorption–emission frequency shift i.e. $g^2N/\kappa \leq \omega_r$, then absorptive transitions will not occur because they are non-resonant and only ($n = 0 \rightarrow n = -1$) transitions, i.e. absorption of pump photons and emission of probe photons, will occur. Consequently, the system evolves in the quantum CARL limit when $G \leq \omega_r$. In contrast, if the spectral width of the SR pulse is sufficiently large (i.e. SR decay is sufficiently rapid) that it is much larger than the absorption–emission frequency difference, so that $G \gg \omega_r$,

then absorptive transitions ($n = 0 \rightarrow n = 1$) will be resonant and both emission and re-absorption of probe photons will occur. Consequently the system evolves in the semiclassical CARL limit when $G \gg \omega_r$. It should be noted that, in contrast to previous explanations [16, 17] of the experimental results in [16], in our argument the duration of the pump pulse is not a significant factor. The reason that the semiclassical CARL or ‘Kapitza–Dirac’ regime can be observed using a short pump pulse in [16] is because the timescale of semiclassical super-radiant decay, $\tau'_{sr} \sim 1/G'$ (see equation (11)), is much shorter than in the ‘super-radiant Rayleigh scattering’ example as a result of the decreased pump–atom detuning. In [16] a suppression of quantum SR gain G of equation (8) by around two orders of magnitude was observed and attributed in [16] to the short duration of the pump pulse. The CARL model described here explains the reduced gain observed in [16] as a result of the fact that the SR scattering process is evolving semiclassically. Consequently, the SR gain is not given by G as given by equation (8) but the semiclassical SR gain G' as given by equation (11). The semiclassical gain, G' , gives a value consistently smaller than the one predicted by the quantum super-radiant gain, G . Using the same parameters as those used in figures 4 and 3, the ratio is $G'/G \approx 0.16$.

6. Conclusion

It has been shown that many features of the recent experiments of Schneble *et al* [16], which show two different regimes of light scattering by the BEC, can be described using a one-dimensional mean-field quantum CARL model. The two regimes of light scattering observed in [16], described as ‘Kapitza–Dirac scattering’ and ‘super-radiant Rayleigh scattering’ in [16], can be interpreted as the semiclassical and quantum limits respectively of CARL lasing. In the semiclassical limit, when $g^2N/\kappa \gg \omega_r$, the collective scattering process involves both absorption and emission of probe photons, and for sufficiently long times many momentum states are populated simultaneously. In the quantum limit, however, when $g^2N/\kappa \leq \omega_r$, the collective scattering process involves emission of probe photons only, and a maximum of two momentum states are populated at any time. We provide a simple explanation of these results in terms of a comparison between the frequency separation of probe emission and absorption events and the spectral width of super-radiant decay between the initial and recoiling condensates. In contrast to previous models of the experiments in [16], the pump pulse duration is not a significant factor in our interpretation. The results presented here support the view of the BEC–light interaction as a strongly coupled atom–optical system where the atoms and light (and consequently the matter–wave and optical gratings) evolve dynamically and self-consistently. This picture gives a more correct and complete description of the interaction than models in which the dynamics of either the atoms (matter–wave grating) or the optical fields (optical grating) are neglected.

References

- [1] Bonifacio R and De Salvo L 1994 *Nucl. Instrum. Methods Phys. Res. A* **341** 360
- [2] Bonifacio R, De Salvo Souza L, Narducci L M and D’Angelo E J 1994 *Phys. Rev. A* **50** 1716

- [3] Bonifacio R, Robb G R M and McNeil B W J 1997 *Phys. Rev. A* **56** 912
- [4] Piovella N, Bonifacio R, McNeil B W J and Robb G R M 2001 *Opt. Commun.* **187** 165
- [5] Piovella N, Gatelli M and Bonifacio R 2001 *Opt. Commun.* **194** 167
- [6] Piovella N, Gatelli M, Martinucci L, Bonifacio R, McNeil B W J and Robb G R M 2002 *Laser Phys.* **12** 188
- [7] Robb G R M, Piovella N, Ferraro A, Bonifacio R, Courteille Ph W and Zimmermann C 2004 *Phys. Rev. A* **69** 041403
- [8] von Cube C, Slama S, Kruse D, Zimmermann C, Courteille Ph W, Robb G R M, Piovella N and Bonifacio R 2004 *Phys. Rev. Lett.* **93** 083601
- [9] Inouye S, Chikkatur A P, Stamper-Kurn D M, Stenger J, Pritchard D E and Ketterle W 1999 *Science* **285** 571
- [10] Kozuma M, Suzuki Y, Torii Y, Sugiura T, Kugam T, Hagley E W and Deng L 1999 *Science* **286** 2309
- [11] Bonifacio R, Cataliotti F S, Cola M, Fallani L, Fort C, Piovella N and Inguscio M 2004 *Opt. Commun.* **233** 155
- [12] Moore M G and Meystre P 1998 *Phys. Rev. A* **58** 3248
- [13] Moore M G, Zobay O and Meystre P 1999 *Phys. Rev. A* **60** 1491
- [14] Mustecaplioglu O E and You L 2000 *Phys. Rev. A* **62** 063615
- [15] Trifonov E D 2002 *Laser Phys.* **12** 211
- [16] Schneble D, Torii Y, Boyd M, Streed E W, Pritchard D E and Ketterle W 2003 *Science* **300** 475
- [17] Pu H, Zhang W and Meystre P 2003 *Phys. Rev. Lett.* **91** 150407
- [18] Piovella N, Salasnich L, Bonifacio R and Robb G R M 2004 *Laser Phys.* **14** 278